

Universality in fermionic dimer-dimer scattering

A. Deltuva*

Institute of Theoretical Physics and Astronomy, Vilnius University, Saulėtekio al. 3, LT-10257 Vilnius, Lithuania

(Received March 12, 2022)

Collisions of two fermionic dimers near the unitary limit are studied using exact four-particle equations for transition operators in momentum space. Universal properties of dimer-dimer phase shifts and effective range expansion (ERE) parameters are determined. The inclusion of the fourth-order momentum term in the ERE significantly extends its validity to higher collision energies. The dimer-dimer scattering length and effective range are determined in the unitary limit as well as their corrections arising due to the finite range of the two-fermion interaction. These results are of considerably higher accuracy as compared to previous works, but confirm most of the previous results except for the lattice effective field theory calculations.

PACS numbers: 34.50.Cx, 31.15.ac, 21.30.-x, 21.45.-v

I. INTRODUCTION

Few-particle systems with large s -wave scattering length a exhibit universal properties independent of the short-range interaction details. One of the most prominent examples is the Efimov effect [1], the emergence of an infinite number of weakly bound three-particle states (trimers) with total orbital angular momentum $L = 0$ and geometric energy spectrum in the unitary limit $a \rightarrow \infty$. Furthermore, there are four-particle (unstable) bound states (tetramers) associated with each trimer [2–5]. However, the Efimov effect is prohibited in the system of identical spin $\frac{1}{2}$ fermions (including both components, i.e., spin up and down states), due to the antisymmetry of the wave function. The only bound state in such a system with large a (assuming the absence of deeply bound states) is a weakly-bound dimer formed by two fermions with antiparallel spins; absolute value of its binding energy is approximately given by $\varepsilon_2 \approx \hbar^2/ma^2$ where m is the fermion mass (unit convention $\hbar = 1$ is adopted in the present work). The total spin, orbital and total angular momentum of the dimer are zero, i.e., in the standard spectroscopic $^{2S+1}L_J$ notation it is realized in the 1S_0 partial wave. Although there are no four-fermion bound states, the four-body physics is important for the properties of cold dilute molecular gases that are determined by the parameters of low-energy dimer-dimer collisions [6–8]. The dimer-dimer scattering length a_{dd} has been investigated in a number of works [6–10], all predicting $a_{dd}/a \approx 0.6$ in the large a limit, but the studies at finite collision energies are scarcer and contradicting [7, 8, 10]. The correlated Gaussian (CG) [7], the fixed-node diffusion Monte Carlo (FN-DMC) [7], and the hyperspherical adiabatic (HA) [8] approaches predict the dimer-dimer effective range r_{dd}/a to be 0.13(2), 0.12(4), and 0.13, respectively, while the recent lattice effective field theory (L-EFT) calculation [10] with thorough systematic error estimation claims a very different result

$r_{dd}/a = -0.431(48)$. One has to admit that most of the above approaches are based on a finite-volume approximation and need extrapolation to get free-space results. This is not needed for the exact formulation of the four-particle scattering problem as proposed by Faddeev and Yakubovsky [11] and by Alt, Grassberger, and Sandhas (AGS) [12]. In the latter case the properly symmetrized equations for the four-particle transition operators have been applied to the study of the four-boson Efimov physics [4, 5, 13]. The AGS equations were solved numerically in the momentum-space partial-wave representation leading to the most accurate results for the bosonic particle-trimer and dimer-dimer scattering processes. The present work aims to extend the methodology of Refs. [4, 5, 13] for the scattering of two fermionic dimers and to provide accurate benchmark results.

Section II contains dimer-dimer scattering equations and some details of calculations, results are reported in Sec. III, and conclusions are presented in Sec. IV.

II. THEORY

The AGS equations [12] in the symmetrized form suitable for the bosonic dimer-dimer scattering were given in Ref. [13]. Using the spin formalism, spin up and down fermions can be considered as different states of identical particles, thereby allowing to consider the system of four identical fermions and antisymmetrize the AGS equations in a corresponding way. Thus, the scattering equations can be generalized to include formally both bosonic and fermionic systems by introducing the symmetry parameter ζ being +1 for bosons and −1 for fermions, i.e.,

$$\mathcal{U}_{12} = (G_0 t G_0)^{-1} + \zeta P_{34} U_1 G_0 t G_0 \mathcal{U}_{12} + U_2 G_0 t G_0 \mathcal{U}_{22}, \quad (1a)$$

$$\mathcal{U}_{22} = (1 + \zeta P_{34}) U_1 G_0 t G_0 \mathcal{U}_{12}. \quad (1b)$$

The four-particle transition operators $\mathcal{U}_{\beta\alpha}$ are labeled according to the two cluster partitions, $\beta = 1$ standing for the 3+1 partition (12,3)4, and $\beta = 2$ standing for the 2+2

* arnoldas.deltuva@tfai.vu.lt

partition (12)(34). The two-particle transition matrix

$$t = v + vG_0t \quad (2)$$

is calculated from the potential v where $G_0 = (E + i0 - H_0)^{-1}$ is the free four-particle resolvent at the available energy E in the center-of-mass (c.m.) frame and H_0 is the free Hamiltonian for the relative motion. Furthermore,

$$U_\beta = P_\beta G_0^{-1} + P_\beta t G_0 U_\beta \quad (3)$$

are the transition operators for the 1+3 and 2+2 subsystems with $P_1 = P_{12} P_{23} + P_{13} P_{23}$, $P_2 = P_{13} P_{24}$ and the permutation operators P_{ab} of particles a and b .

The AGS equations (1) are solved in the momentum-space partial-wave framework where they become a system of integral equations with three continuous variables, the magnitudes of the Jacobi momenta k_x , k_y and k_z [14]; the associated orbital angular momenta are l_x , l_y , and l_z . As compared to the bosonic spin zero case [4, 5, 13, 14], the basis states have to be extended to include the spins $s_i = \frac{1}{2}$. The states of the total angular momentum \mathcal{J} with projection \mathcal{M} are $|k_x k_y k_z \{l_z \{l_y \{l_x (s_1 s_2) s_x\} j_x s_3\} S_y\} J_y s_4\} S_z\} \mathcal{J} \mathcal{M}\rangle$ for the 3+1 configuration and $|k_x k_y k_z (l_z \{l_x (s_1 s_2) s_x\} j_x [l_y (s_3 s_4) s_y] j_y\} S_z) \mathcal{J} \mathcal{M}\rangle$ for the 2+2 configuration; the calculation of U_β is performed in the corresponding basis while transformations from one basis to another are needed in certain steps of the solution process [15]. The discrete quantum numbers j_x and j_y are the total angular momenta of pairs (12) and (34), J_y is the total angular momentum of the (123) subsystem, and s_x , s_y , S_y , and S_z are the intermediate subsystem spins. To ensure the full antisymmetry of the four-fermion system, the basis states must be antisymmetric under exchange of two fermions in the subsystem (12) for the 3 + 1 partition and in (12) and (34) for the 2 + 2 partition, i.e., $l_x + s_x$ (and $l_y + s_y$ for the 2 + 2 configuration) must be even. When solving equations (1) numerically, the integrals are discretized using Gaussian quadratures. The absence of near-threshold $\mathcal{U}_{\beta\alpha}$ poles allows for an accurate solution using iterative methods such as the double Padé summation of Ref. [15]. Thus, there is no necessity for the direct matrix inversion and separable form of v , t , U_β , and $\mathcal{U}_{\beta\alpha}$ as used in the four-boson calculations [4, 5, 13, 14]. Below the dimer breakup threshold the only singularity in the kernel arises from the dimer-dimer pole in U_2 ; it is treated by the subtraction method [15]. The partial-wave amplitude for the elastic dimer-dimer scattering with the relative on-shell momentum p_{dd} and $E = -2\varepsilon_2 + p_{dd}^2/2m$ is obtained as

$$\mathcal{T}_{dd}^{\mathcal{J}}(p_{dd}) = 2\langle\phi_2^{\mathcal{J}}(p_{dd})|\mathcal{U}_{22}|\phi_2^{\mathcal{J}}(p_{dd})\rangle \quad (4)$$

where $|\phi_2^{\mathcal{J}}(p_{dd})\rangle = G_0 t P_2 |\phi_2^{\mathcal{J}}(p_{dd})\rangle$ is the \mathcal{J} -component of the Faddeev amplitude of the asymptotic channel state $|\Phi_2(\mathbf{p}_{dd})\rangle = (1 + P_2)|\phi_2(\mathbf{p}_{dd})\rangle$. Given the symmetry restrictions, only even \mathcal{J} contribute to the dimer-dimer

scattering; furthermore, for each \mathcal{J} the Faddeev amplitude $|\phi_2^{\mathcal{J}}(p_{dd})\rangle$ has a single component with $l_x = s_x = j_x = l_y = s_y = j_y = S_z = 0$ and $l_z = \mathcal{J}$. The scattering amplitude (4) leads to the single-channel S -matrix and phase shift $\delta_{\mathcal{J}}$ as

$$\mathcal{S}_{dd}^{\mathcal{J}}(p_{dd}) = e^{2i\delta_{\mathcal{J}}} = 1 - 2i\pi m p_{dd} \mathcal{T}_{dd}^{\mathcal{J}}(p_{dd}). \quad (5)$$

Further details of the numerical methods used to solve the AGS equations can be found in Ref. [15].

III. RESULTS

To study the universality in fermionic dimer-dimer collisions and to prove the independence of the short-range interaction details, three types of potential models are used in the present work; all of them are assumed to act in the s -wave $l_x = 0$ only. The first one is a separable potential $v(k'_x, k_x) = g(k'_x) \lambda g(k_x)$ with Gaussian form factors $g(k_x) = e^{-(k_x/\Lambda)^2}$. The cutoff parameter Λ and the strength λ are adjusted to reproduce the desired values of two-fermion scattering length a and effective range r_e . The second type corresponds to a fictitious four-neutron system with enhanced two-neutron interaction supporting a weakly bound dineutron. For this purpose a realistic charge-dependent Bonn (CD Bonn) potential [16] multiplied by a factor ranging from 1.1 to 1.17 is used; such a variation is sufficient to control the dimensionless ratio r_e/a that characterizes the deviation from the unitary limit. In a similar way, the third type corresponds to a fictitious system of ^3He atoms interacting through the modified LM2M2 potential [17] multiplied by a factor around 1.3; the transformation to the momentum space is performed as described in Ref. [18] taking $r_{\min} = 2.3$ fm and $r_{\max} = 50$ fm. In the following the three potential types will be labeled Vsep, CDBx, and LM2M2x, respectively. Since all models differ also in ε_2 , the collision energy will be characterized by another dimensionless quantity ap_{dd} ; the dimer breakup threshold corresponds to $ap_{dd} \approx \sqrt{2}$.

The calculated phase shifts δ_0 and δ_2 are presented in Fig. 1. The latter remains very small over the whole energy regime; thus, the dimer-dimer scattering is strongly dominated by the relative s -wave. The results are shown for six different a/r_e values ranging from 16 to 127; only the curves for lower a/r_e are discernible, indicating that higher a/r_e predictions approximate well the unitary limit results.

It is important to evaluate also the theoretical error bars. They are dominated by the truncation of the partial-wave expansion for the 3+1 configuration and by the numerical accuracy of integrations and interpolations when solving the scattering equations. The results in Fig. 1 include orbital angular momenta l_y and l_z up to 4, i.e., J_y up to $\frac{9}{2}$. Reducing to $l_y, l_z \leq 3$, $J_y \leq \frac{7}{2}$ changes δ_0 by 0.005 deg at most, while increasing to $l_y, l_z \leq 5$, $J_y \leq \frac{11}{2}$ leads to changes by 0.001 deg or less. The number of momentum discretization grid points increases

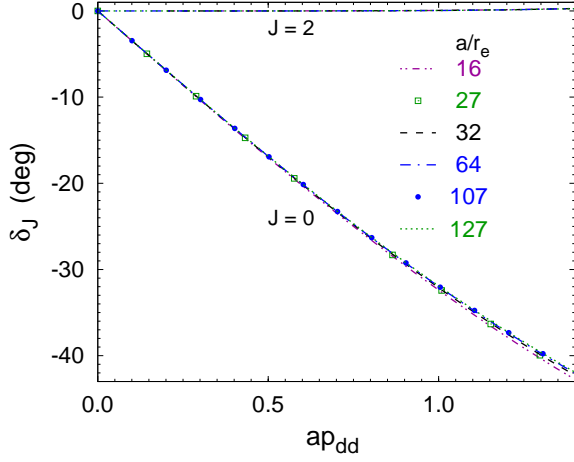


FIG. 1. (Color online) Phase shifts for fermionic dimer-dimer scattering in s and d waves. Results are obtained for different ratios a/r_e using the models Vsep (curves), CDBx (full circles), and LM2M2x (boxes).

from 30 (for lowest a/r_e) to 70 (for highest a/r_e); the δ_0 predictions are stable within 0.001 to 0.005 deg for reasonable variations of grid point distributions. Due to the presence of significant high-momentum components, the accuracy is lower in LM2M2x calculations. Otherwise, the theoretical error bars for the phase shift results are well below 0.01 deg, enabling an accurate extraction of the effective range expansion (ERE) parameters. To extend the validity of the ERE to higher collision energies, fourth-order momentum term is included, i.e.,

$$ap_{dd} \cot \delta_0 \approx -\frac{a}{a_{dd}} + \frac{1}{2} \frac{r_{dd}}{a} (ap_{dd})^2 - \frac{1}{4} c_{dd} (ap_{dd})^4. \quad (6)$$

The importance of this term is illustrated in Fig. 2, comparing directly calculated $ap_{dd} \cot \delta_0$ and its ERE. The second-order ERE at $ap_{dd} > 0.5$ deviates from the exact results while the fourth-order ERE fits the exact results very well over the considered energy regime $ap_{dd} < 1.4$.

The convergence of the dimensionless ERE parameters a_{dd}/a and r_{dd}/a towards the unitary limit is studied in Fig. 3. The predictions for a number of Vsep (curves), CDBx (full circles), and LM2M2x (boxes) models are plotted as functions of the respective r_e/a values. The CDBx results include the uncertainties resulting from the ERE fit procedure. They are 0.0002 for a_{dd}/a and 0.001 for r_{dd}/a . The error bars are the same for Vsep predictions but are not shown, while LM2M2x predictions have larger error bars. Within given error bars the agreement between Vsep, CDBx, and LM2M2x results is perfect, indicating the independence of the short range interaction details. a_{dd}/a and r_{dd}/a to a good accuracy correlate with r_e/a linearly at $r_e/a < 0.04$, enabling not only a reliable extrapolation to the unitary limit but also a systematic evaluation of finite range effects. Taking into account Vsep and CDBx results with the error bar estimation from all uncertainty sources, the relations are

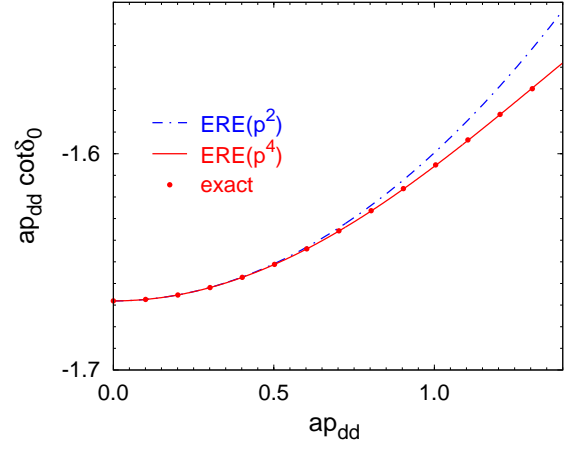


FIG. 2. (Color online) Function $ap_{dd} \cot \delta_0$, calculated directly at $a/r_e \approx 127$, is compared with its ERE with/without the fourth-order momentum term.

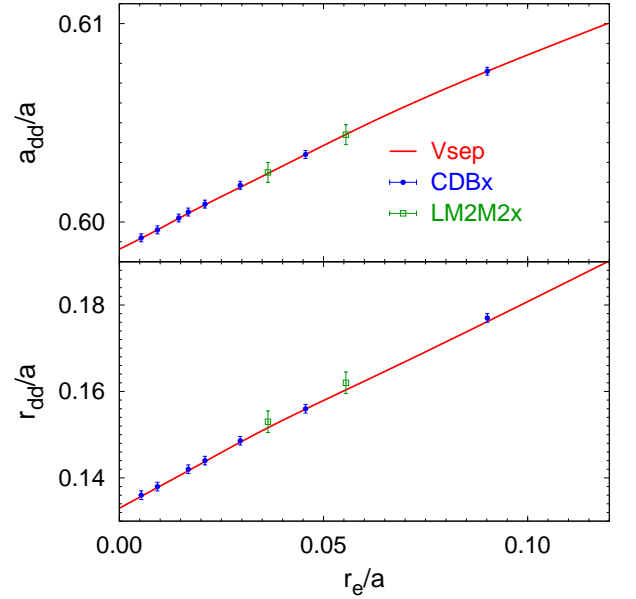


FIG. 3. (Color online) Dimer-dimer scattering length and effective range near the unitary limit calculated using Vsep (curves), CDBx (full circles), and LM2M2x (boxes) models.

$$\frac{a_{dd}}{a} = 0.5986 + 0.105 \frac{r_e}{a} \pm 0.0005, \quad (7a)$$

$$\frac{r_{dd}}{a} = 0.133 + 0.51 \frac{r_e}{a} \pm 0.002. \quad (7b)$$

The fourth-order ERE coefficient c_{dd} is small and has relatively large uncertainty, i.e.,

$$c_{dd} = 0.026 - 0.1 \frac{r_e}{a} \pm 0.004. \quad (7c)$$

On a relative scale, r_{dd} and c_{dd} exhibit substantially stronger r_e dependence than a_{dd} , i.e., as one could ex-

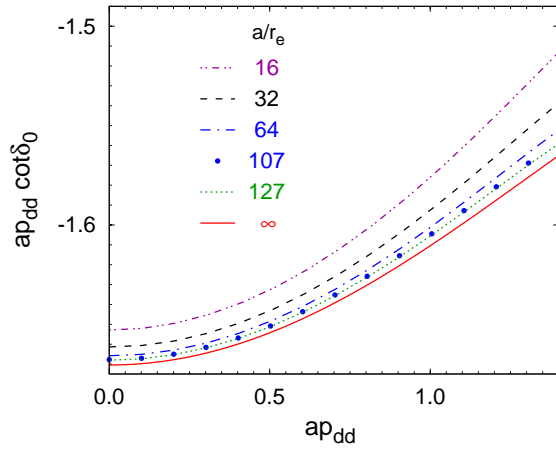


FIG. 4. (Color online) Function $ap_{dd} \cot \delta_0$ for finite a/r_e values is compared with its unitary limit (solid curve) calculated using parameters from Eqs. (7).

pect, the importance of finite range effects increases with increasing collision energy. This can be seen clearly also in Fig. 4, comparing $ap_{dd} \cot \delta_0$ results for a number models with finite a/r_e and the unitary limit ERE: the spread of predictions becomes wider with increasing ap_{dd} .

IV. SUMMARY

Fermionic dimer-dimer scattering near the unitary limit was studied using exact four-particle equations for transition operators that were solved numerically in the momentum-space partial-wave framework. Three types

of interaction models were used proving the independence of the results of the short-range potential details and thereby establishing universal behaviour of dimer-dimer phase shifts and ERE parameters. The usual ERE up to the second-order in momentum was found to be valid for low collision energies only, but including the fourth-order term $\frac{1}{4}c_{dd}(ap_{dd})^4$ as in Eq. (6) extends the ERE validity up to the dimer breakup threshold. The finite range r_e of the two-fermion interaction leads to corrections for a_{dd}/a , r_{dd}/a , and c_{dd} that, sufficiently close to the unitary limit, are linear in r_e/a as given in Eqs. (7); furthermore, the finite range correction increases with increasing collision energy.

The present results are of considerably higher accuracy as compared to previous works. All of them are consistent with the present value of the dimer-dimer scattering length in the unitary limit, $a_{dd}/a = 0.5986 \pm 0.0005$. The obtained effective range parameter $r_{dd}/a = 0.133 \pm 0.002$ supports previous CG, FN-DMC, and HA calculations of Refs. [7, 8] and indicates heavy failure of the L-EFT method [10]. Since the lattice-type methods become used quite often, especially in nuclear physics, it is very important to evaluate their reliability for scattering calculations.

Regarding the nuclear physics, the present work considers a fictitious four-neutron system with bound dineutrons. Nevertheless, this is an important step towards the study of tetra-neutron states using realistic interactions.

The author acknowledges the support by the Alexander von Humboldt-Stiftung and the hospitality of the Ruhr-Universität Bochum where a part of this work was performed.

-
- [1] V. Efimov, Phys. Lett. B **33**, 563 (1970).
 - [2] H. W. Hammer and L. Platter, Eur. Phys. J. A **32**, 113 (2007).
 - [3] J. von Stecher, J. P. D’Incao, and C. H. Greene, Nature Phys. **5**, 417 (2009).
 - [4] A. Deltuva, Phys. Rev. A **82**, 040701(R) (2010).
 - [5] A. Deltuva, Europhys. Lett **95**, 43002 (2011).
 - [6] D. S. Petrov, C. Salomon, and G. V. Shlyapnikov, Phys. Rev. Lett. **93**, 090404 (2004).
 - [7] J. von Stecher, C. H. Greene, and D. Blume, Phys. Rev. A **77**, 043619 (2008).
 - [8] J. P. D’Incao, S. T. Rittenhouse, N. P. Mehta, and C. H. Greene, Phys. Rev. A **79**, 030501 (2009).
 - [9] A. Bulgac, P. F. Bedaque, and A. C. Fonseca, arXiv:cond-mat/ 0306302 (2003).
 - [10] S. Elhatisari, K. Katterjohn, D. Lee, U.-G. Meißner, and G. Rupak, Phys. Lett. B **768**, 337 (2017).
 - [11] O. A. Yakubovsky, Yad. Fiz. **5**, 1312 (1967) [Sov. J. Nucl. Phys. **5**, 937 (1967)].
 - [12] P. Grassberger and W. Sandhas, Nucl. Phys. **B2**, 181 (1967); E. O. Alt, P. Grassberger, and W. Sandhas, JINR report No. E4-6688 (1972).
 - [13] A. Deltuva, Phys. Rev. A **84**, 022703 (2011).
 - [14] A. Deltuva, Phys. Rev. A **85**, 012708 (2012).
 - [15] A. Deltuva and A. C. Fonseca, Phys. Rev. C **75**, 014005 (2007).
 - [16] R. Machleidt, Phys. Rev. C **63**, 024001 (2001).
 - [17] R. A. Aziz and M. J. Slaman, J. Chem. Phys. **94**, 8047 (1991).
 - [18] A. Deltuva, Few-Body Syst. **56**, 897 (2015).